

A Digital Output Piezoelectric Accelerometer for Ultra-low Power Wireless Sensor Node

Toshihiro Itoh, Takeshi Kobayashi, Hironao Okada
National Institute of Advanced Industrial Science and
Technology (AIST),
1-2-1, Namiki, Tsukuba, Japan, 305-8564
toshihiro-itoh@aist.go.jp
CREST, JST, Japan

Takashi Masuda, Tadatomo Suga
Dept. Precision Engineering, The University of Tokyo,
7-3-1, Hongo, Bunkyo-ku, Tokyo, Japan, 113-8656
CREST, JST, Japan

Abstract— We have developed a novel piezoelectric accelerometer with digital output for ultra-low power wireless sensor nodes. The accelerometer is composed of an array of piezoelectric parallel-plate capacitor structures that are joined together in series and connected to a CMOS switch array. This composition makes it possible to realize a digital output accelerometer in which the number of on-state CMOS switches increases with increasing acceleration. The switches can be turned on by the voltage generated due to the piezoelectric effect and then the acceleration can be directly converted to digital output without an A/D converter. In this study, we have designed this type of accelerometer and developed its fabrication process utilizing SOI wafer and sol-gel derived PbZrTiO_3 (PZT) thin films. And a wireless sensor node integrated with the fabricated accelerometer device has been demonstrated. Evaluating the devices, it has been shown that an ultra-low power accelerometer can be realized with improving the piezoelectric property of the piezoelectric thin film.

I. INTRODUCTION

A ubiquitous sensor network is composed of a large number of distributed wireless microsensor nodes that are attached or embedded to humans or things and sense their conditions or environmental information around them automatically. And it is used to take measures to meet the sensed situation. The sensor networks are expected to be applied to the systems for realizing safe and secure society, human health monitoring and so on. The wireless sensor node, consisting of sensors, a transceiver (or transmitter), supporting electronics and a battery, has been dramatically improved in its performance and functions and miniaturized thanks to recent advance in micro electro mechanical systems (MEMS) technology. The MEMS technology is also expected to contribute to realization of autonomous sensor nodes without batteries by providing a small high-efficient energy harvesting device.

As one of the important applications of sensor network technologies, we have been developing a global avian

influenza surveillance system by monitoring the health of chickens with wireless sensor nodes in poultry farms [1]. The Asian lineage of highly pathogenic avian influenza (HPAI) virus (H5N1) was first detected in Southern China in 1996. The H5N1 virus infection in birds has continued for 12 years in Asia, and has acquired increased pathogenicity not only in birds but also in mammals [2]. The more cases of migratory birds and domestic fowls increase, the more human cases increase and the variation of the virus progresses. Consequently, risks of occurrence of a pandemic flu with transmissibility among humans increase. Therefore a global avian influenza surveillance system for the early-stage detection of birds cases must be effective to defend human beings from an influenza pandemic.

One of the key issues for the design of wireless sensor nodes is power [3-5]. For the global avian influenza surveillance system, the nodes should work continuously for periods of longer than one year without battery replacement. Since the weigh including a battery should be less than 1 g and the shape must be a small band-aid one for this chicken health monitoring application, an upper limit of the power consumption could be less than 10 μW for each node. In order to reduce the power consumption of the nodes, which will include a body temperature sensor and accelerometer as an activity sensor, the power consumption of the accelerometer should be drastically reduced. In our application, it is not necessary to detect the acceleration with high accuracy, but it may be enough to sense when the acceleration is over some thresholds, for instance. In this study, we propose an ultra-low power piezoelectric accelerometer with digital output for such kind of applications.

While piezoelectric accelerometers have been used mostly for vibration or shock measurements, piezoelectric MEMS accelerometer using piezoelectric thin films have been developed over a quarter of a century [6-10]. Recently, in addition, the piezoelectric MEMS is expected to be a promising energy harvesting MEMS device [11,12]. In this

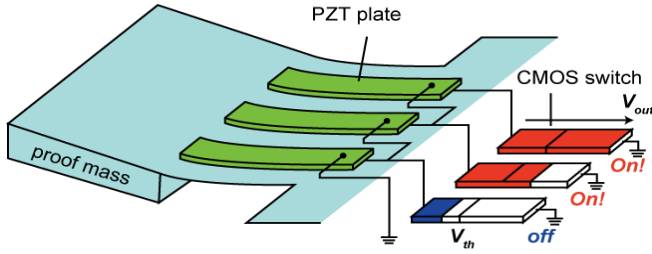


Fig. 1 Schematic illustration of the concept of the digital output accelerometer. In this figure, 2 CMOS switches are on-state.

paper, a novel accelerometer with the following advantages is proposed and demonstrated:

- 1) It can work with zero power consumption due to the piezoelectric effect.
- 2) It is utilized for an event-driven type sensor node that wakes up from a sleep-state only when the acceleration is over a threshold.
- 3) Digital output is generated without an A/D converter.

II. CONCEPT & DESIGN

Fig. 1 illustrates the concept of the digital output accelerometer. The accelerometer is composed of an array of piezoelectric PZT parallel-plate capacitor structures on a Si microcantilever. The PZT structures are joined together in series and connected to a CMOS switch array. Due to the piezoelectric effect, the number of on-state CMOS switches increases with increasing acceleration. This composition makes it possible to realize a digital output accelerometer in which output is the number of on-state CMOS switches.

Fig. 2 shows the dimensions of the designed accelerometer with 10 PZT parallel-plate capacitor structures. The dimensions of the cantilever and the proof mass are $5000 \times 8000 \times 5 \mu\text{m}$ and $5000 \times 5000 \times 500 \mu\text{m}$, respectively. If the load (mass \times acceleration) is applied at center of gravity of the proof mass, the approximate output voltage generated from a PZT plate can be derived by

$$V = \frac{d_{31} E_{PZT} F}{K_f} w_{Ti/Pt/Ti} \left\{ y_n - \left(h_{SiO_2} + h_{Ti/Pt/Ti} + \frac{h_{PZT}}{2} \right) \right\} \left\{ \frac{l_{Ti/Pt/Ti}^2}{2} + \alpha l_{Ti/Pt/Ti} \right\} \quad (1)$$

$$\varepsilon_{PZT} \frac{w_{Ti/Pt/Ti} l_{Ti/Pt/Ti}}{h_{PZT}} + C_0$$

where d_{31} , E_{PZT} , ε_{PZT} and h_{PZT} are the piezoelectric coefficient, young module, relative dielectric constant and height of PZT film, K_f is the bending rigidity of the cantilever, F is the load applied at the proof mass, y_n is the distance to the neutral axis of the cantilever, α is the distance between the top of the cantilever and the center of gravity of the cantilever, C_0 is the capacitance of a CMOS switch, $w_{Ti/Pt/Ti}$, $h_{Ti/Pt/Ti}$ and $l_{Ti/Pt/Ti}$ are width, height and length of the Ti/Pt/Ti layer, and h_{SiO_2} is the height of the SiO_2 layer.

The estimated output voltage of one PZT plate per 1 G is about 53 mV_{pp} . If a CMOS switch with the threshold

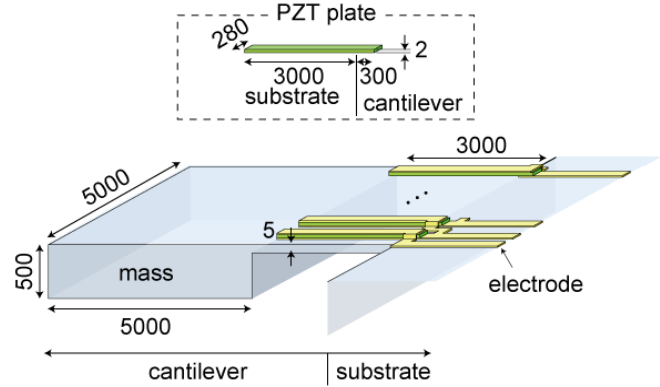


Fig. 2 The dimensions of the designed cantilever. The unit is μm .

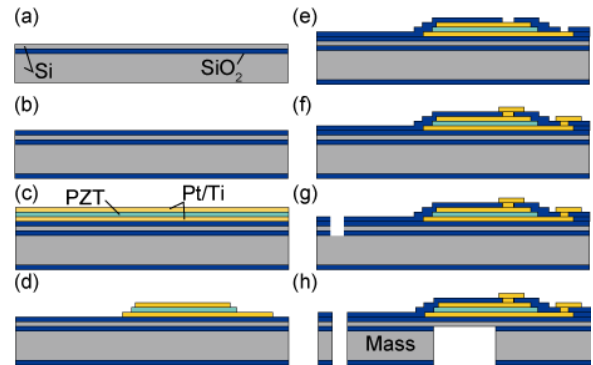


Fig. 3 The fabrication process of the accelerometer.

voltage of 0.3 V is used, for instance, the CMOS switch is turned on by the output voltage of 12 PZT plates joined together in series

III. FABRICATION PROCESS

Fig. 3 depicts the fabrication process. SOI wafers with an $5 \mu\text{m}$ thick (100)-oriented structural Si layer and a $1 \mu\text{m}$ thick buried oxide (BOX) layer were used as the substrates (Fig. 3(a)). The deposition of a multilayer of Pt/Ti/PZT/Pt/Ti/ SiO_2 began with the thermal oxidation of the SOI wafer at 1373 K to form $0.54 \mu\text{m}$ thick SiO_2 thin films (Fig. 3(b)). Next, as shown in Fig. 3(c), Pt/Ti thin films ($175 \text{ nm}/5 \text{ nm}$ in thickness) were sputtered at 373 K as the bottom electrode. Then, $2 \mu\text{m}$ thick (100)-oriented PZT thin films were deposited by chemical solution deposition using layer-by-layer crystallization multi-coating process. Commercially available PZT solution (PZT-20; Kojundo Chemical Co, Japan) was used as a precursor solution. The Pb/Ti/Zr composition was set at a molar ratio of 1.2:0.52:0.48. The solution was spin-coated onto the substrate at 3200 rpm and pyrolyzed at 523 K . Then, the films were crystallized by rapid thermal annealing (RTA 10 K/s) at 973 K for 2 min . These steps were repeated 16 times to obtain the $2 \mu\text{m}$ thick PZT film, before top electrodes of Ti/Pt/Ti thin films ($5 \text{ nm}/175 \text{ nm}/5 \text{ nm}$ in thickness)

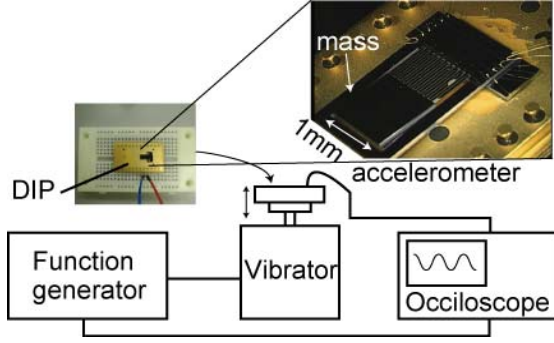


Fig. 4 Schematic illustration of experimental setup.

were sputtered at 373 K. The top and bottom Pt/Ti electrodes and PZT films were patterned by Ar ion beam etching and removed by wet etching with an aqueous solution of BHF/HNO₃/HCl, respectively (Fig. 3(d)). Consequently, the 800 nm thick SiO₂ layer for insulation between the top and bottom electrodes was deposited by sputtering at 573 K and the windows for interconnection were opened by reactive ion etching (RIE) using CHF₃ gas (Fig. 3(e)). After the Pt/Ti interconnection layer were deposited and patterned (Fig. 3(f)), the thermal SiO₂ thin films, structural Si and BOX layer were etched using RIE, where the etching gases were CHF₃ for SiO₂ and SF₆ for Si (Fig. 3(g)). Finally, the Si substrate and BOX layer were etched from the backside by deep RIE to release the cantilever (Fig. 3(h)).

IV. EVALUATION RESULTS AND DISCUSSION

Fig.4 illustrates the schematic images of the measurement setup for evaluation of the fabricated accelerometers. The fabricated accelerometer is attached to a dual inline package (DIP), whose output pins are connected to the input of an oscilloscope directly. By attaching the board with the accelerometer to the vibrator, the accelerometer can be oscillated by the vibrator which receives sinusoidal wave signals generated by a function generator. Since the wiring patterns from each bottom electrodes were prepared, the output of each PZT plate could be measured.

Fig. 5 (a) shows the remnant polarization and voltage outputs of as-fabricated PZT films. The horizontal axis represents the PZT plate number. If the phase of the output voltage is almost reverse of the input voltage, the output voltage is negative. The dispersion indicates that the fabrication process damaged piezoelectric films and deteriorated the piezoelectric property. However, as shown in Fig. 5 (b), 450 °C annealing with 30 minutes successfully made the property uniform. The average of the output voltages per a PZT film plate is measured as 8.9 mV_{pp}/g, while the theoretical output is 3 - 5 times larger than the measured one. In order to increase the output, the properties of PZT film could be improved by optimizing the micromachining process [13], for instance.

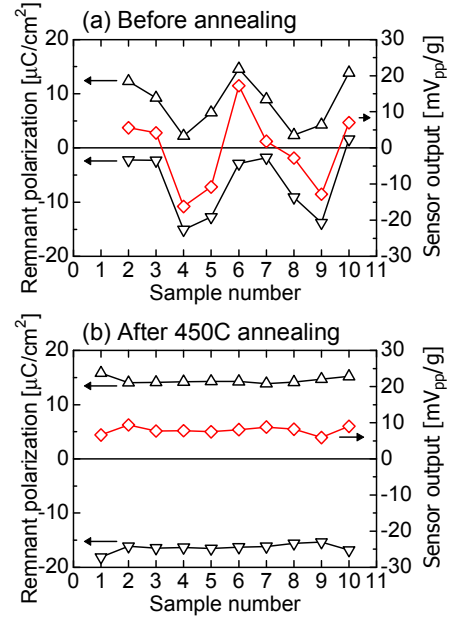


Fig. 5 Effectiveness of 450°C, 30 minutes annealing (a) before annealing, and (b) after annealing

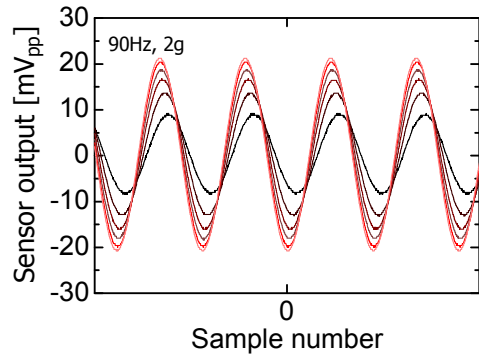


Fig. 6 Sensor output voltage from 1, 2, 3, 4 and 5 PZT plates joined in series, respectively.

Fig. 6 shows the sensor output voltage curves from 1, 2, 3, 4 and 5 PZT plates joined in series, respectively, when the acceleration with the amplitude of 2 G and the frequency is 90 Hz was applied. Although the concept that the voltage increases with the number of PZT plates can be confirmed, the voltage does not increase linearly. It is also found that the phase delay occurs as the number of plates increases. Further investigation is necessary to clarify the cause.

Fig. 7 (a) shows a wireless sensor node integrated with the fabricated accelerometer device. The output voltages of the accelerometer are amplified, then the signals are transmitted by a wireless module after the voltages are converted into digital signals by an A/D converter in the wireless module. Fig. 7 (b) shows the output voltages

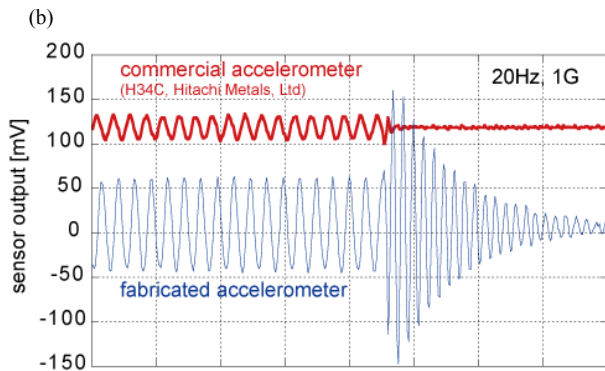
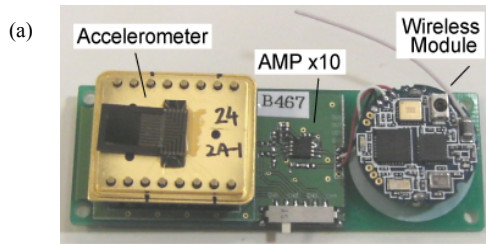


Fig. 7 (a) Prototype wireless node with the fabricated and a commercial accelerometer. The output voltage of the fabricated accelerometer is amplified by $\times 10$ amplifier. (b) The output voltages of the fabricated and commercial accelerometers when the acceleration with the amplitude of 1 G and the frequency is 20 Hz was applied.

of the fabricated and a commercial accelerometer (H34C, HITACHI Metals Ltd.) in the wireless module when the acceleration with the amplitude of 1 G and the frequency is 20 Hz was applied and stopped in the middle of the measurement. Although the damping of the vibration of the fabricated accelerometer was slow, the output voltages were almost the same as the commercial accelerometer.

V. SUMMARY

We have proposed a digital output piezoelectric accelerometer without A/D converter for ultra low power wireless sensor nodes and developed a fabrication process for its prototype. It has been demonstrated that the fabricated device can work as expected in principle, while it has been found that average of the output voltages per a PZT film plate is as small as $8.9 \text{ mV}_{pp}/g$ and the voltage of PZT plates joined in series does not increase linearly.

ACKNOWLEDGEMENT

This research is supported by fund of the CREST (Core Research for Evolutional Science and Technology) of JST (Japan Science and Technology Agency). The authors would like to thank Mr. Y. Yushita for his contributions to the device fabrication during his master's course in the University of Tokyo.

REFERENCES

- [1] http://www.jst.go.jp/kisoken/crest/intro/pdf/crest_eng_2007-2008Dec.pdf
- [2] http://www.who.int/csr/disease/avian_influenza/en/index.html
- [3] C. Ó Mathúna, T. O'Donnell, R. V. Martinez-Catala, J. Rohan, and B. O'Flynn, "Energy scavenging for long-term deployable wireless sensor networks," *Talanta*, vol. 75, 2008, pp. 613-623
- [4] I. F. Akyildiz, W. Su, Y. Sankarasubramaniam, E. Cayirci, "Wireless sensor networks: a survey," *Computer Networks*, vol. 38, 2002, pp. 393-422
- [5] B. H. Calhoun, et al., *IEEE Trans. Computer* 54 (2005) 727-740
- [6] P. L. Chen and R. S. Muller, "Integrated Silicon PI-FET Accelerometer with Proof Mass," *Sensors and Actuators*, vol. 5, 1984, pp. 119-126
- [7] S. P. Beeby, J. N. Ross, and N. M. White, "Design and fabrication of a micromachined silicon accelerometer with thick-film printed PZT sensors," *J. Micromech. Microeng.*, vol. 10, 2000, pp. 322-328
- [8] K. Kunz, P. Enoksson, G. Stemme, "Highly sensitive triaxial silicon accelerometer with integrated PZT thin film detectors," *Sensors and Actuators A*, vol. 92, 2001, pp. 156-160
- [9] Q.-M. Wang, Z. Yang, F. Li, and P. Smolinski, "Analysis of thin film piezoelectric microaccelerometer using analytical and finite element modeling," *Sensors and Actuators A*, Vol. 113, 2004, pp. 1-11
- [10] Q. Zou, W. Tan, E. S. Kim, and G. E. Loeb, "Single- and Triaxis Piezoelectric-Bimorph Accelerometers," *J. Microelectromechanical Systems*, vol. 17, 2008, pp. 45-57
- [11] S. Roundy, P. K. Wright, and J. Rabaey, "A study of low level vibrations as a power source for wireless sensor nodes," *Computer Communications*, vol. 26, 2003, pp. 1131-1144
- [12] S. P. Beeby, M. J. Tudor, and N. M. White, "Energy harvesting vibration sources for Microsystems applications," *Meas. Sci. Technol.*, vol. 17, 2006, pp. R175-R195
- [13] T. Kobayashi et al., Degradation in the ferroelectric and piezoelectric properties of $\text{Pb}(\text{Zr,Ti})\text{O}_3$ thin films derived from a MEMS microfabrication process, *J. Micromech. Microeng.* 17, 1238-1241